Geophys. J. Int. (2003) **154,** 1–7

Slip partitioning in the Sea of Marmara pull-apart determined from GPS velocity vectors

F. Flerit,[1] R. Armijo,[1] G. C. P. King,[1] B. Meyer[1] and A. Barka[2]

[1] *Laboratoire de Tectonique, Institut de Physique du Globe,* 4 *place Jussieu, Paris,* 75252, *France, Cedex* 05
[2] *Department of Geology, Istanbul Technical University, Ayazaga, Istanbul, Turkey*

Accepted 2002 October 24. Received 2002 August 26; in original form 2002 April 3

SUMMARY

Dislocation modelling is used to examine the GPS velocity vectors for the Marmara Sea region. First, the vectors due to the known Anatolia/Eurasia rotation are reproduced by introducing structures that approximate the large-scale tectonics. Observed features of the smaller scale fault system in the Marmara region are then progressively included with slip amplitudes and directions adjusted to fit an 80-vector subset of the GPS data. The motion in the Marmara Sea region is partitioned with the faults that bound the north of the basin carrying more strike-slip motion than predicted from the Anatolia-Eurasia plate motion and faults to the south having a greater perpendicular component. Taken together however, there is no net opening across the Marmara Sea perpendicular to the overall trend of the boundary and thus deformation in the Marmara region results only from the pull-apart geometry of the North Anatolian fault. No extension related to the Aegean system is needed to explain the observations. The GPS results are consistent with motion over the last 5 Myr that has been determined from geological reconstructions.

Key words: elastic-plastic lithosphere, GPS field, interseismic deformation, Marmara Sea, pull apart, slip partitioning, Tectonics.

INTRODUCTION

Over the last decade numerous GPS sites have been established throughout Turkey and Greece resulting in progressively better determination of the velocity vectors describing interseismic crustal deformation for the region (Straub *et al.* 1997; Kahle *et al.* 2000; McClusky *et al.* 2000). Such deformation can now be compared with rates determined by geological and geomorphic methods over longer time periods (e.g. Barka 1992; Armijo *et al.* 1996, 1999; Hubert-Ferrari *et al.* 2002a). This paper concentrates on the Sea of Marmara region, which has excited interest following the 1999 Izmit and Düzce earthquakes. Further destructive events are to be expected in the near future (Barka 1999; Parsons *et al.* 2000; Hubert-Ferrari *et al.* 2000). The Sea of Marmara lies on, or close to, the boundary between the strike-slip Anatolian regime and the Aegean region which includes substantial N–S extension (Le Pichon & Angelier 1981; Jackson *et al.* 1992). To help to understand how the Anatolian and Aegean tectonic regimes have influenced the evolution of the Marmara Sea, we examine present-day motion using GPS observations.

Most of the GPS velocity vectors relative to Eurasia can be explained by rotation of Anatolia and the Aegean around an Euler pole (McClusky *et al.* 2000). However two regions show misfits that fall outside the errors of observation—much of the Southern Aegean and the region of the Sea of Marmara. Although this paper concentrates on the Sea of Marmara, we start by creating a large scale model that incorporates the major active structures and reproduces the results (including defects) of using a simple pole of rotation. Within the context of this model, the Sea of Marmara velocity vectors are then examined using a knowledge of the faults with known Holocene activity (Barka & Kadinsky-Cade 1988; Saroglu *et al.* 1992; Parke *et al.* 1999; Le Pichon *et al.* 2001; Armijo *et al.* 1999, 2002). It is assumed that these faults are the surface expression of deeper structures which are then modelled by dislocation elements in a half-space; a common approach to modelling GPS data (Savage & Burford 1973). Recent work has assumed that these structures divide a region into blocks and use procedures that minimise strains within them (e.g. McClusky *et al.* 2001; Meade *et al.* 2002). This procedure however, can result in motion on a structure being incompatible with surface observations (e.g. closure on an extensional feature). Our models do not require the blocks to be undeforming, but do require that the direction of the horizontal component of slip vectors on the structures that we model are compatible with geological (Barka & Kadinsky-Cade 1988; Saroglu *et al.* 1992; Parke *et al.* 1999; Le Pichon *et al.* 2001; Armijo *et al.* 1999, 2002) and seismological observations (e.g. Ambraseys & Jackson 2000; Gurbuz *et al.* 2000). The significance of deformation within blocks is discussed by Hubert-Ferrari *et al.* (2002b).

THE SEA OF MARMARA FAULT SYSTEM

To the east of the Sea of Marmara, the North Anatolian fault (NAF) has a single trace where deformation has been limited to a narrow zone over several million years (Fig. 1a) (Hubert-Ferrari *et al.* 2002a). At the eastern end of the Sea of Marmara, the fault splits into two systems, the North, North Anatolian Fault (NNAF) and the South, North Anatolian Fault (SNAF). The NNAF passes through the Marmara Sea to the Dardanelles while the SNAF passes on land to the South (Fig. 2a). The NNAF is substantially more active than the SNAF. The strike-slip deformation on both then continues into the Aegean where it interacts with extension that has been active for the last 15 Myr. In Fig. 1(a) the general form of the earlier and still active Aegean extension is indicated in yellow. As the two branches of the NAF extend into the Aegean, activity is reduced on its eastern side and increased to the west (dark green). The North Aegean Trough, Evvia and Corinth basins (Fig. 1a) result from the increased activity (Armijo *et al.* 1996).

The NAF appears to have evolved by propagation from east to west (Armijo *et al.* 1996; Hubert-Ferrari *et al.* 2002a,b). It initiated in Eastern Turkey between 15 and 10 Ma as a result of the collision of Arabia and Eurasia and crossed the western Marmara Sea at 5 Ma (Armijo *et al.* 1999). Further propagation has resulted in the reactivation of the Gulf of Corinth at 1 Ma (Armijo *et al.* 1996). It is this propagation process that is responsible for reducing activity on the eastern side of the fault and increasing it to the west (Hubert-Ferrari *et al.* 2002b).

Within this context the Marmara Basin has evolved over the last 5 Ma mainly as a result of strike-slip motion and it can be identified kinematically as a pull-apart (in the offset between the NAF and the NNAF) with some minor complexities (Armijo *et al.* 2002). These geological reconstructions suggest that, while Aegean extension may play some initial role in creating the Sea of Marmara structures, overall extension perpendicular to the overall trend of the NAF is not required to reconstruct the geology. The GPS modelling reported below supports this view.

GPS OBSERVATIONS AND LARGE SCALE MODELLING

The GPS observations on which this study is based are shown in Fig. 1(a) (Eurasia fixed) and the area of detailed study is outlined. Elements of a regional model that fits these observations are shown in Figs 1(b) and (c). They consist of rectangular elements that extend from a locking depth of 15 km to 100 000 km (effectively infinite depth) in an elastic half space (Poisson's ratio 0.25). This simulates vertical structures that extend through the lower crust and upper mantle to the asthenosphere (Savage & Burford 1973). Deformation is calculated using the results for rectangular dislocations of Okada (1985). The green elements which represent the NAF are simplified and continued as far as the Hellenic arc. Thus the complexities of the southern Aegean are not fully modelled. The initial model (Fig. 1c) does not include the SNAF and all motion is placed on the NNAF. The normal and tangential motion on the elements are such that the net slip vector has the amplitude and direction predicted by the Anatolia/Eurasia kinematics ($\sim$24 mm yr^{-1} McClusky *et al.* 2000). The Hellenic subduction system is modelled by blue elements and yellow elements represent some of the extensional features in Western Turkey and the Aegean. The vectors are consistent with geological rates and produce an overall velocity field consistent with the larger scale plate motions (determined from the pole of rotation). As previously noted this initial model provides a poor fit for the Southern Aegean, but this does not affect further modelling in Marmara Sea region.

DETAILED MODELLING IN THE SEA OF MARMARA

Fig. 2(a) shows the known active faults of the Marmara region (Barka & Kadinsky-Cade 1988; Saroglu *et al.* 1992; Armijo *et al.* 2002) together with the GPS vectors referenced to Eurasia. In Fig. 2(b) the initial model (as in Fig. 1) is shown allowing the GPS vectors and the model vectors to be compared. The model fits the vectors to the north of the NNAF and in the southern part of the region shown (about 100 km to the south of the Marmara Sea). The good fit surrounding the Marmara region is important since it shows that there is no overall extension perpendicular to the NAF.

Closer to the Marmara Sea, substantial differences occur. While it is easier to understand the whole region when vectors are referenced to Eurasia, the significance of vectors in the immediate Marmara region is clearer when referenced to Anatolia (Fig. 2c). In this figure it can be seen that many vectors are orientated approximately perpendicular to the overall direction of motion on the boundary. The following Figs 3(a), (b), (c) and (d) show steps required to fit these vectors.

In each figure the upper panel shows observed and predicted velocity vectors. The central panel shows the elements, the slip vectors on the elements and the model velocities. The residuals in the lower panel are indicated both by vectors and by an interpolated and shaded error field. The latter makes it easy to see where misfits are greatest. This is a reliable method for identifying systematic errors in groups of vectors and hence for systematically improving a model. A global rms misfit represented by a single number gives little guide to how a model can be improved.

For the initial model (Fig. 3a) it can be seen that errors result from incorrect modelling of the velocity component perpendicular to the Anatolia/Eurasia motion, plus some error parallel to the strike of that motion. It should be appreciated that this result is not very sensitive to the exact location of the NNAF. Provided that the model is constrained to accommodate large-scale relative motions, the misfit will have the same general character. This insensitivity is illustrated in Fig. 3(b) where 20 per cent of the slip ($\sim$5 mm yr^{-1}) required by the large-scale kinematics ($\sim$24 mm yr^{-1}) is transferred from the NNAF to the SNAF. This modification reduces the strike-parallel errors but the systematic strike-perpendicular error vectors remain.

To produce a better fit to the observed deformation field it is necessary to reduce extension across structures within the northern Marmara Sea and increase extension to the South. To achieve this, the directions and amplitudes of some of the vectors are changed and opening elements are added as shown in Fig. 3(c) (middle panel). The residuals are substantially reduced. The extension added south of the Sea of Marmara is consistent with geological observations indicating that significant normal faulting occurs (Barka & Kadinsky-Cade 1988; Saroglu *et al.* 1992; Armijo *et al.* 2002). The fit consequently requires slip partitioning with a larger proportion of strike-slip motion accommodated on the NNAF and strike-perpendicular extension associated with the SNAF and associated faults. The model reduces almost all of the residuals to well within the error ellipses and can thus be regarded as good fit.

However, pursuing the observation that substantial extension occurs south of the Sea of Marmara and not within it, models can be produced that reduce the residuals still further. A satisfactory model

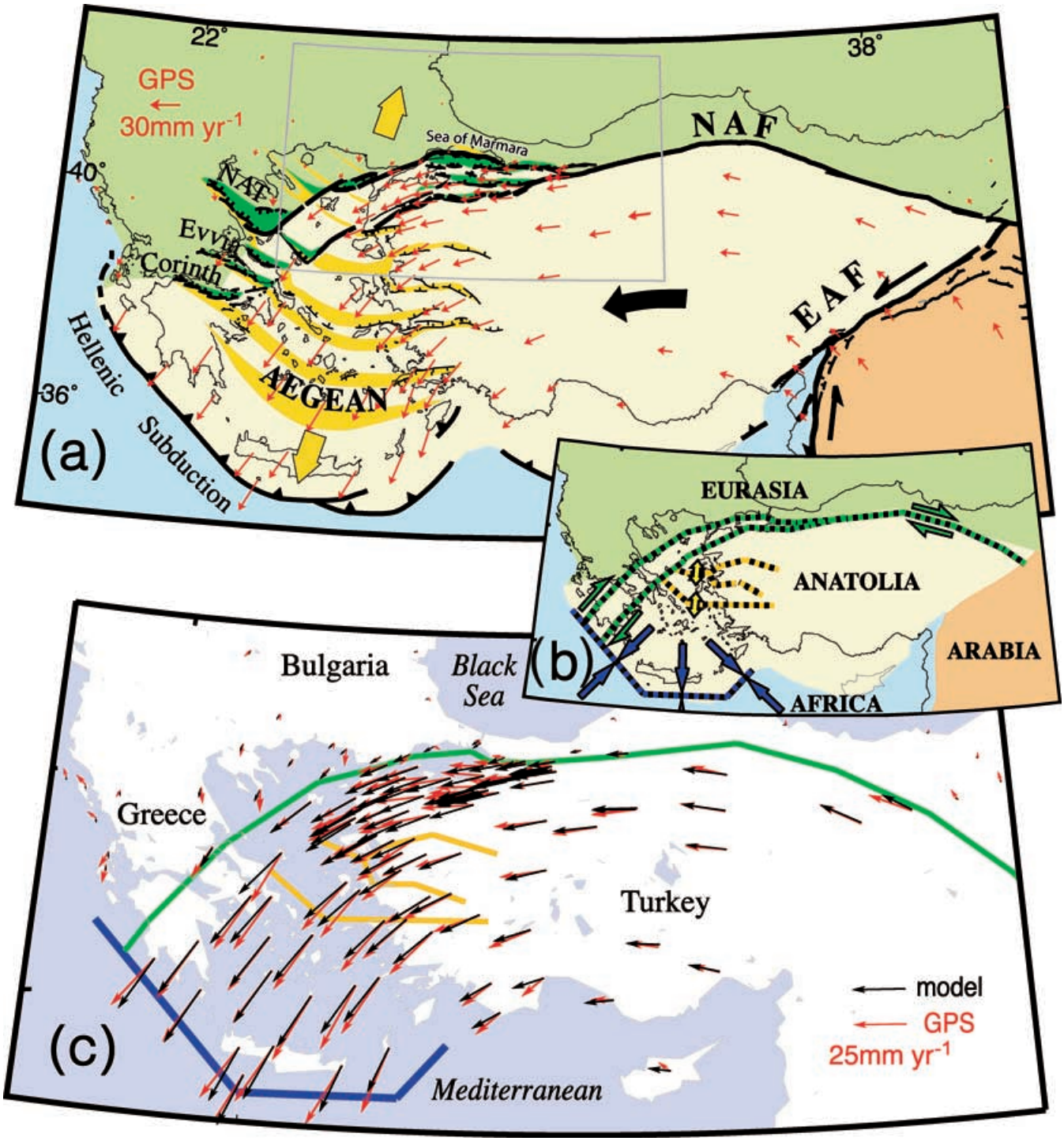

Figure 1. Tectonic setting of the Sea of Marmara in the eastern Mediterranean. (a) The Anatolian block escapes to the east as a result of the collision between Eurasia and Arabia. The block is bounded to the North by the North Anatolian fault (NAF), to the east by the East Anatolian fault (EAF) and to the south by the Hellenic subduction zone. In the west, the NAF interacts with the extensional system of the Aegean. Yellow features indicate structures that have been active in the last 15 Myr and yellow arrows indicate the overall extension direction. The structures shown in dark green have been re-activated by the NAF propagating into the region. Red arrows are GPS vectors referenced to a fixed Eurasia taken from McClusky *et al.* (2000). (b) The structures used in this paper to model the overall GPS velocity field. The modelled NAF is indicated in green. The blue structures model closure due to subduction with directions indicated by blue arrows. The yellow structures are extensional as indicated by divergent yellow arrows. The location of these features is compatible with structures known to accommodate Quaternary deformation. These structures are part of a second study to fit velocity vectors throughout the Aegean. However, for this study, only those features necessary to model deformation vectors in the Marmara region and to produce a good fit to the rotation model of McClusky *et al.* (2000) are used. (c) The initial model reproducing the overall Anatolia/Eurasia kinematics. The NAF is modelled with a single trace in the Aegean. The fits to the data are very close around the Marmara region. The model is only approximate for Southern Greece, the Southern Aegean and SW Turkey.

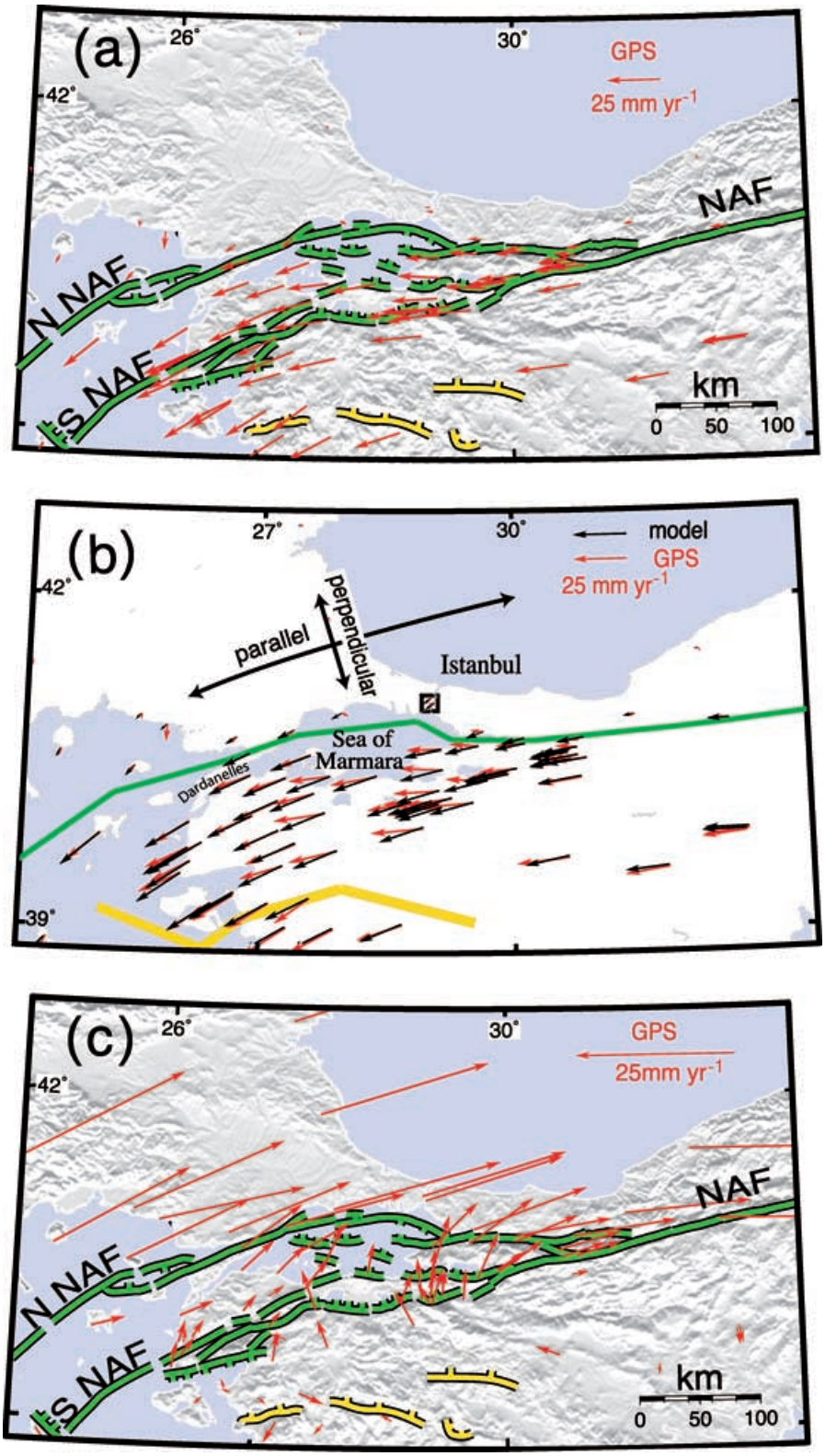

Figure 2. (a) The Marmara region showing the mapped faults (Barka & Kadinsky-Cade 1988; Saroglu *et al.* 1992; Armijo *et al.* 2002) and the 80 GPS velocity vectors for the region (referenced to fixed Eurasia). The NAF splays westwards into two main branches 100 km apart (NNAF, SNAF, see text). The Marmara pull-apart basin has formed at the step-over between the NAF to the East and the NNAF to the West. Note that the NNAF is more active (4–5 times) than the SNAF. (b) The same region as in (a) showing the initial model with only the NNAF included (close-up of Fig. 1c). The vectors at a distance from the Marmara Sea are well fitted, but those to the immediate south are not well modelled. The directions parallel and perpendicular to the overall Anatolia motion are outlined by double-headed arrows. (c) Mapped faults and GPS vectors referenced to fixed Anatolia (obtained by removing the Anatolia/Eurasia rotation of McClusky *et al.* 2000). Velocities in the Marmara region include components of motion parallel and perpendicular to the Anatolia motion. Deformation appears mostly restricted to the area between the NNAF and the SNAF.

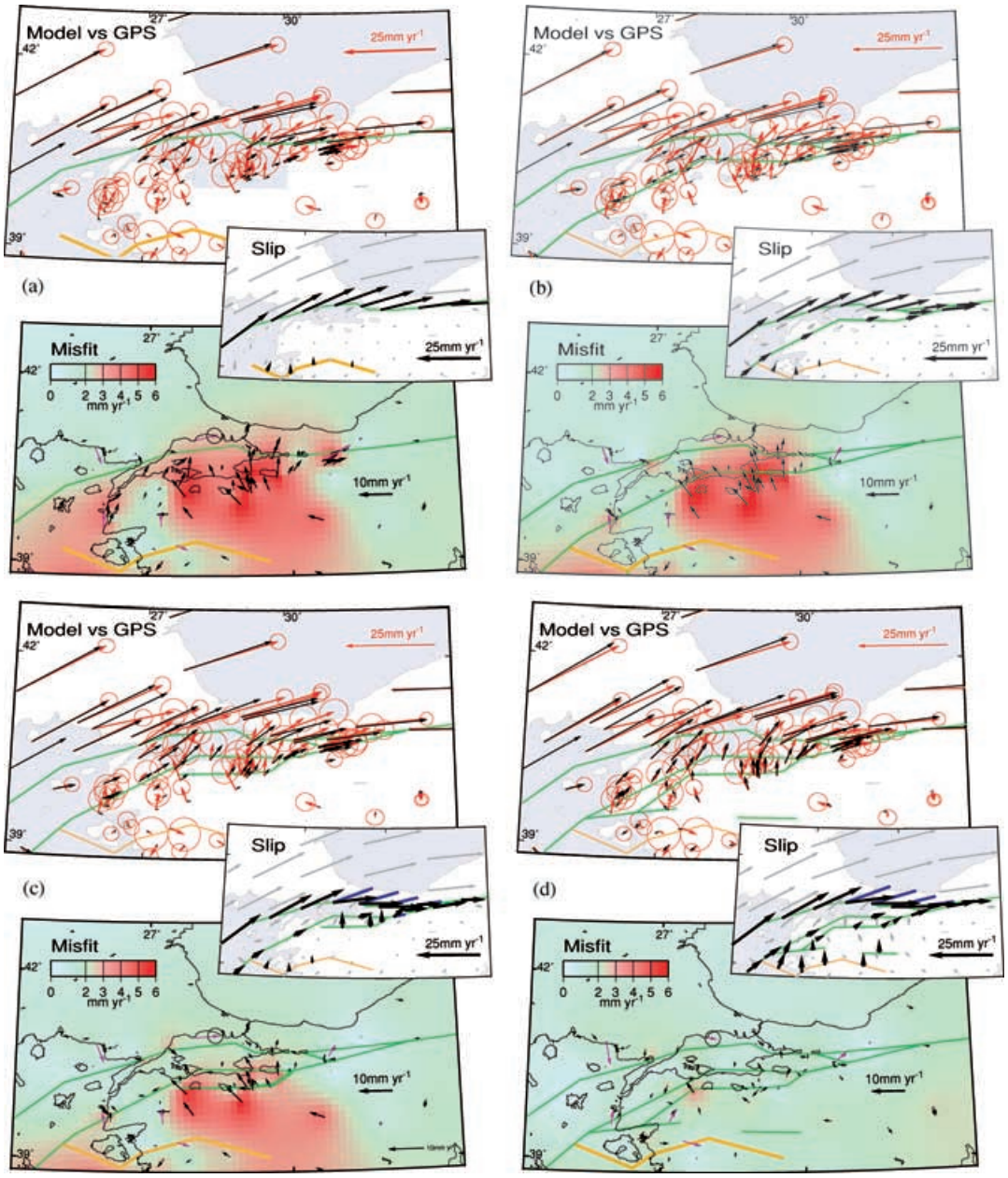

Figure 3. Progressive models of the GPS vectors around the Sea of Marmara. Motion is referenced to fixed Anatolia (as in Fig. 2c). Each figure is composed of three windows. The upper compares the modelled vectors (black) with the observed vectors (red). The ellipses are 80 per cent confidence limits from McClusky *et al.* (2000). The middle window shows the slip vectors (in black) for different parts of the fault system within the region. In all cases, the models include the larger scale structures shown in Fig. 1(b) and the resultant motions are illustrated with grey arrows. The lower window shows the residual vectors (in black) plus shading (in red) indicating the degree of misfit. The latter is calculated by interpolating between scalar values of the misfit. A few vectors (10 out of 90) are either incoherent with other nearby vectors or have a large error. These are indicated in purple and are not included in the calculation of misfit. The arrowhead of one vector, which is not fitted by the first models, is circled. It might be accounted for by adjusting the locking depth (see text). (a) Only the NNAF is modelled with slip everywhere parallel to and with the amplitude predicted by, the plate motion. Large residuals are visible south of the fault. In the west these are parallel to the plate motion while further east they are orientated perpendicular to it. (b) The SNAF is introduced and the plate motion is redistributed with 80 per cent on the NNAF and 20 per cent on the SNAF. Again the slip is everywhere parallel to the plate motion. The residuals to the south and west of the fault are now reduced, but the misfits to the south of the Sea of Marmara remain. (c) Slip on the NNAF is modified to reduce the component of opening along the eastern part of the Marmara Sea. The overall plate motion direction is shown by blue lines and the new slip direction by black arrows. This leaves a slip deficit with a fault perpendicular component, which is re-distributed along normal faults south of the Sea of Marmara as indicated. This slip partitioning between the two branches of the NAF substantially reduces the residuals. They are now sufficiently small to be within the error ellipses. (d) An optimised model. The condition that no changes can be made to the regional model is now relaxed and some other local faults are added. The strike-slip component on the SNAF is slightly increased and this slip increase extends outside the region of interest to include part of the regional model. Within the region, normal faults with modest opening are added. The locking depth for the NNAF in the northern Sea of Marmara is reduced to 5 km with the result that the vector with the circled head, north of the Marmara, is fitted better. The modifications are discussed in the text and can be justified as consistent with more general tectonic interpretations of the region. However, the residuals are now below the errors quoted for the GPS velocity vectors and thus the interpretation presented in this figure may change as more data is collected.

is shown in Fig. 3(d). This adds motion consistent with structures beneath some minor mapped faults and slightly modifies slip on a structure to the south. The details of this model are poorly constrained however, and it may not be fully supported in the future as errors in the velocity vectors are progressively reduced as more GPS data accumulates. The locking depth for structures along the northern Marmara Sea are reduced to 5 km. This slightly improves the fit for one velocity vector (arrowhead circled).

DISCUSSION AND CONCLUSIONS

We have first produced an overall model of the regional displacement field for Western Turkey and the Aegean, consistent with the large-scale kinematics of the extrusion of Anatolia and with geological features known to be active. This correctly describes the displacement field around the Marmara Sea, but closer to it the fit to the data is poor. To fit the observations better, slip partitioning is required with opening across the northern Sea of Marmara reduced and extension to the south of the Sea of Marmara enhanced. There is geological evidence for this asymmetric slip partitioning. The faults along the northern side of the Marmara Sea have greater strike-slip motion than predicted from the pole of rotation while south of the Marmara Sea the faults have larger than predicted normal components. Reconstructions suggest that the deficit of normal motion in the north is compensated by the excess in the south so that taken together the structures do not represent any departure of the horizontal velocity vector from that predicted by the pole of rotation (Armijo *et al.* 2002).

It has been proposed that the Sea of Marmara results from the interaction of Anatolian strike-slip with Aegean extension (Wong *et al.* 1995; Parke *et al.* 1999). Kinematically this does not appear to be the case. Although Aegean style extension does cause motion on E–W normal faults about 100 km to the south of the Sea of Marmara and in the Aegean Sea to the west of the Dardanelles, there is no overall extension perpendicular to the slip direction between the north of the Marmara Sea and about 100 km to the south of it. Within this zone all the perpendicular motions are local and associated with the offset geometry. The geology, morphology and GPS results are therefore in agreement; subsidence due to strike-parallel extension and partitioned slip has formed the basin and continues to enlarge it.

Although the data exclude substantial Aegean extension as playing a significant role in the finite deformation of the Marmara Sea region, the form of the faulting in the region can still have been influenced by the Aegean stress field. While too small to create structures with significant displacements, the Aegean stress field may have modified the evolution of the NAF. As the NAF propagated into the Proto-Marmara Sea area at 5 Ma, N–S extensional stresses would rotate the maximum shear towards the North causing the fault to veer to form the NNAF. Once formed this structure could have controlled the subsequent evolution of the plate boundary in this region. It is however, not kinematically an ideal boundary. The younger and less active SNAF more closely follows the small circle about the pole of rotation and may in due course become the favoured locus of future deformation.

ACKNOWLEDGMENTS

This work is part of the collaborative programme on the seismic risk in the Istanbul and Sea of Marmara region co-ordinated by the Turkish TUBITAK and the French INSU-CNRS, with support from the French Ministry of Foreign Affairs (MAE) and INSU IT programme Dynamique de la fracturation Lithospherique. This is Institut de Physique du Globe de Paris (IPGP) paper No. 1860. INSU paper No. 342.

REFERENCES

Ambraseys, N.N. & Jackson, J.A., 2000. Seismicity of the Sea of Marmara (Turkey) since 1500, *Geophys. J. Int.,* **141,** F1–F6.

Armijo, R., Meyer, B., King, G.C.P., Rigo, A. & Papanastassiou, D., 1996. Quaternary evolution of the Corinth Rift and its implication for the late Cenozoic evolution of the Aegean, *Geophys. J. Int.,* **126,** 11–53.

Armijo, R., Meyer, B., Hubert, A. & Barka, A., 1999. Westwards Propagation of the North Anatolian Fault into the Northern Aegean: Timing and kinematics, *Geology,* **27,** 267–270.

Armijo, R., Meyer, B., Navarro, S., King, G. & Barka, A., 2002. Asymmetric slip partitioning in the Sea of Marmara pull-apart: A clue to propagation processes of the North Anatolian fault?, *TerraNova,* **14,** 80–86.

Barka, A., 1992. The North Anatolian fault zone, *Ann. Tectonicae,* **6,** 164–195.

Barka, A., 1999. The 17 August 1999 Izmit Earthquake, *Science,* **285,** 1858–1859.

Barka, A. & Kadinsky-Cade, K., 1988. Strike-slip fault geometry in Turkey and its influence on earthquake activity, *Tectonics,* **7,** 663–684.

Gurbuz, C. *et al.*, 2000. The seismotectonics of the Marmara region (Turkey): results from a microseismic experiment, *Tectonophysics,* **316,** 1–17.

Hubert-Ferrari, A., Barka, A., Jacques, E., Nalbant, S., Meyer, B., Armijo, R., Tapponnier, P. & King, G.C.P., 2000. Seismic hazard in the Marmara Sea following the 17 August 1999 Izmit earthquake, *Nature,* **404,** 269–272.

Hubert-Ferrari, A., Armijo, R., King, G.C.P., Meyer, B. & Barka, A., 2002a. Morphology, displacement and slip rates along the North Anatolian Fault (Turkey), *J. geophys. Res.,* 2002, **107,** B10, ETG9-1–ETG-33.

Hubert-Ferrari, A., King, G.C.P., Manighetti, I., Armijo, R., Meyer, B. & Tapponnier, P., 2002b. Long-term Elasticity in the Continental Lithosphere; Modelling the Aden Ridge Propagation and the Anatolian Extrusion Process, *Geophys. J. Int.,* 2003, **153,** 111–132.

Jackson, J.A., Haines, J. & Holt, W., 1992. The horizontal velocity field in the deforming Aegean Sea region determined from the moment tensor of earthquakes, *J. geophys. Res.,* **97,** 17 657–17 684.

Kahle, H.G., Cocard, M., Peter, Y., Geiger, A., Reilinger, R., Barka, A. & Veis, G., 2000. GPS-derived strain rate field within the boundary zones of the Eurasian, African, and Arabian Plates, *J. geophys. Res.,* **105,** 23 353–23 370.

Le Pichon, X. & Angelier, J., 1981. The Aegean Sea, *Phil. Trans. R. Soc. Lond., A,* **300,** 357–372.

Le Pichon, X. *et al.*, 2001. The active main Marmara fault, *Earth planet. Sci. Lett.,* **192,** 595–616.

McClusky, S. *et al.*, 2000. Global Positioning System constraints on the plate kinematics and dynamics in the eastern Mediterranean and Caucasus, *J. geophys. Res.,* **105,** 5695–5719.

McClusky, S.C., Bjornstad, S.C., Hager, B.H., King, R.W., Meade, B.J., Miller, M.M., Monastero, F.C. & Souter, B.J., 2001. Present day kinematics of the eastern California shear zone from a geodetically constrained block model, G.R.L., 28, Vol. 17, pp. 3369–3372.

Meade, J.B., Hager, B.H., McClusky, S.C., Reilinger, R.E., Ergintav, S., Lenk, O., Barka, A. & Özener, H., 2002. Estimates of seismic potential in the Marmara Sea region from block models of secular deformation constrained by global positioning system measurements, *Bull. seism. Soc. Am.,* **92,** 208–2015.

Okada, Y., 1985. Surface deformation to shear and tensile faults in a half space, *Bull. seism. Soc. Am.,* **75,** 1135–1154.

Parke, J.R. *et al.*, 1999. Active faults in the Sea of Marmara, western Turkey, imaged by seismic reflection profiles, *TerraNova,* **11,** 223–227.

Parsons, T., Toda, S., Stein, R.S., Barka, A. & Dieterich, J.H., 2000. Heightened odds of large earthquakes near Istanbul: An interaction-based probability calculation, *Science,* **288,** 661–665.

Saroglu, F., Emre, O. & Kuscu, I., 1992. Active Fault Map of Turkey, General Directorate of Mineral Research and Exploration (MTA), Eskisehir Yolu, 06520, Ankara, Turkey.

Savage, J. & Burford, R., 1973. Geodetic determination of relative plate motion in Central California, *J. geophys. Res.,* **78,** 832–845.

Straub, C., Khale, H.-G. & Schindler, C., 1997. GPS and geologic estimates of tectonic activity in the Marmara Sea region, NW Anatolia, *J. geophys. Res.,* **102,** 27 587–27 601.

Wong, H.K., Lüdmann, E., Ulug, T. & Görür, N., 1995. The sea of Marmara: a boundary sea in an escape tectonic regime, *Tectonophysics,* **244,** 231–250.